A Real-Time Non-invasive Auto-bioluminescent Urinary Bladder Cancer Xenograft Model

Bincy Anu John[1], **Tingting Xu**[2], **Steven Ripp**[2,3], and **Hwa-Chain Robert Wang**[1,2]

[1]Department of Biomedical and Diagnostic Sciences, College of Veterinary Medicine, University of Tennessee, Knoxville, TN, USA

[2]Center for Environmental Biotechnology, University of Tennessee, Knoxville, TN, USA

[3]490 BioTech, Inc., Knoxville, TN, USA

Abstract

Purpose—The study was to develop an auto-bioluminescent urinary bladder cancer (UBC) xenograft animal model for pre-clinical research.

Procedure—The study used a humanized, bacteria-originated lux reporter system consisting of six (luxCDABEfrp) genes to express components required for producing bioluminescent signals in human UBC J82, J82-Ras, and SW780 cells without exogenous substrates. Immune-deficient nude mice were inoculated with Lux-expressing UBC cells to develop auto-bioluminescent xenograft tumors that were monitored by imaging and physical examination.

Results—Lux-expressing auto-bioluminescent J82-Lux, J82-Ras-Lux, and SW780-Lux cell lines were established. Xenograft tumors derived from tumorigenic Lux-expressing auto-bioluminescent J82-Ras-Lux cells allowed a serial, non-invasive, real-time monitoring by imaging of tumor development prior to the presence of palpable tumors in animals.

Conclusions—Using Lux-expressing auto-bioluminescent tumorigenic cells enabled us to monitor the entire course of xenograft tumor development through tumor cell implantation, adaptation, and growth to visible/palpable tumors in animals.

Keywords

Auto-bioluminescence; Urinary bladder cancer; *In vivo* imaging; Mouse model

---

Introduction

Bioluminescence imaging (BLI) is a real-time, non-invasive technology to detect implanted, viable bioluminescent cells *in vivo*; one application of this technology is to monitor cancer cell-derived xenograft tumor development in animals [1]. We used a bacteria-originated lux reporter system, consisting of six genes (*luxCDABEfrp*) whose protein products are capable of synthesizing all components necessary to produce a bioluminescent signal autonomously [2–4]. We developed a *PiggyBac* transposon-based delivery vector pPBCMV$_{Lux}$ to facilitate integration of the lux gene cassette into host cell chromosomes for stable expression of lux gene products in viable cells [4].

UBC is the fifth most common human cancer in the USA (www.bcan.org). Immunotherapy, chemotherapy, radiation, and surgery are routinely used to control UBC; however, these therapies are still not optimal. Thus, it is imperative to advance pre-clinical models for developing therapeutic strategies to effectively control UBC. In this report, we describe the generation of Lux-expressing human UBC J82-Lux, J82-Ras-Lux, and SW780-Lux cell lines *in vitro*. It was reported that oncogenic H-Ras is activated in more than 35 % of UBCs [5]. Thereafter, we used the auto-bioluminescent J82-Ras-Lux cells to study the course of tumor development *in vivo*.

Materials and Methods

Cell Culture and Reagents

Human J82, SW780 (American Type Culture Collection [ATCC], Rockville, MD, USA), and oncogenic H-Ras(V12)-expressing, J82-Ras cells [6] were maintained in DMEM supplemented with 10 % FBS. Cultures were maintained in medium supplemented with 100 U/ml penicillin and 100 μg/ml streptomycin in 5 % CO_2 at 37 °C.

Expression Vectors and Auto-bioluminescent Cell Lines

The transposon-based delivery vector pPBCMV$_{Lux}$ vector was constructed by insertion of the CMV promoter and the *luxCDABEfrp* gene cassette, which were isolated from the pCMV$_{Lux}$ vector [4], into the sequence between the N- and C-terminal PiggyBac inverted terminal repeats in the transposon vector PB-Neo (Transposagen Biopharmaceuticals, Lexington, KY, USA). Cells were co-transfected with pPBCMV$_{Lux}$ and the PiggyBac transposase expression vector sPBo (Transposagen Biopharmaceuticals). After transfection, Lux-expressing cell clones were selected with G418 and imaged with the IVIS Lumina system (Perkin Elmer, Waltham, MA, USA) to identify auto-bioluminescent J82-Lux, J82-Ras-Lux, and SW780-Lux cell lines.

Examination of Auto-bioluminescent Xenograft Tumors

J82-Ras-Lux cells were mixed with Matrigel basement membrane matrix (BD Biosciences, San Jose, CA, USA) and injected subcutaneously into 5-week-old female athymic nu/nu mice (Charles River, Wilmington, MA, USA). Mice were placed in an anesthetic chamber and imaged with the IVIS Lumina system; auto-bioluminescent intensity of inoculated cells was measured photons per second (ph/s). Bioluminescent images were analyzed using

Living Image 4.3.1 software (Perkin Elmer). After euthanasia of mice by exposure to CO_2, xenograft tumors were harvested, fixed in neutral-buffered formalin, and embedded in paraffin, followed by hematoxylin and eosin (H&E) staining of tissue sections for histopathological examination. All animal procedures were approved by the University of Tennessee Animal Care and Use Committee and were in accordance with the NIH Guide for the Care and Use of Laboratory Animals.

Immunoblotting

Equal amounts of cellular proteins were resolved by electrophoresis in 12 % SDS-polyacrylamide gels and transferred to nitrocellulose membranes for immunoblotting, using specific antibodies and to detect H-Ras, phosphorylated Erk (p-Erk), Erk, VEGF, β-actin (Santa Cruz Biotechnology, Santa Cruz, CA, USA), phosphorylated Mek (p-Mek), Mek, phosphorylated Akt (p-Akt), and Akt (Cell Signaling, Danvers, MA, USA), as described previously [7]. Antigen–antibody complexes on membranes were detected by the Supersignal chemiluminescence kit (Pierce, Rockford, IL, USA).

Statistical Analysis

Data of bioluminescence images were plotted as mean bioluminescence (ph/s) and analyzed with standard errors of the mean (SEM).

Results

Development of Auto-bioluminescent Human Bladder Cancer Cell Lines

Auto-bioluminescent J82-Lux, J82-Ras-Lux, and SW780-Lux cell lines were developed from cell clones that expressed the highest levels of BLI signals among isolated clones survived from G418 selection. Various numbers of J82-Lux, J82-Ras-Lux, and SW780-Lux cells were plated and imaged with the IVIS Lumina system to determine levels of BLI signals (Fig. 1a, c, e). Analysis of bioluminescent images revealed that J82-Lux cells yielded bioluminescence of 0.207×10^6, 1.143×10^6, and 1.864×10^6 ph/s with 5×10^4, 50×10^4, and 500×10^4 cells, respectively (Fig. 1b). J82-Ras-Lux cells yielded 0.512×10^6, 2.358×10^6, and 4.26×10^6 ph/s with 5×10^4, 50×10^4, and 500×10^4 cells, respectively (Fig. 1d). SW780 cells yielded bioluminescence of 0.217×10^6 and 0.45×10^6 ph/s with 50 and 500 ($\times 10^4$) cells, respectively (Fig. 1f). Accordingly, J82-Ras-Lux cells expressed higher BLI levels than J82-Lux and SW780-Lux cells. In addition, we did not detect any changes of ectopically-expressed H-Ras nor the downstream Mek-Erk and Akt pathways in J82-Ras-Lux cells versus J82-Ras, (Fig. 1g) by additional ectopic expression of the *lux* reporter gene cassette. Thus, we continued to use J82-Ras-Lux cells for the following *in vivo* studies.

In Vivo BLI of J82-Ras-Lux Cells and Derived Tumors

To determine the minimal population of auto-bioluminescent cells required for BLI detection *in vivo*, J82-Ras-Lux cells were implanted subcutaneously into nude mice. After 3 days of cell implantation, mice were imaged; only the J82-Ras-Lux cells inoculated at 500×10^4 were detectable with a bioluminescence of 5.10×10^5 ph/s at the inoculation site (Fig. 2a). However, bioluminescence was not detectable in animals inoculated with 550×10^4 or 50×10^4 J82-Ras-Lux cells until 31 and 13 days after inoculation, respectively (Fig. 2a, b).

By day 13, A bioluminescence of 1.42×10^5 ph/s was detected in the inoculated site, without a visible tumor, in the animal inoculated with 500×10^4 cells; by day 31, the animal had developed a large tumor ($1.2 \times 1.0 \times 0.8$ cm) with a bioluminescence of 4.27×10^5 ph/s (Fig. 2a, b).

The animal inoculated with 50×10^4 cells had a bioluminescence of 0.205×10^5 ph/s in the absence of a visible tumor by day 13, and by day 31, the animal had developed a tumor ($0.8 \times 0.8 \times 0.5$ cm) with a bioluminescence of 1.61×10^5 ph/s. Bioluminescence was not detectable in the animal that was inoculated with 5×10^4 cells until day 31 when a visible tumor (0.4-cm diameter) developed with a bioluminescence of 0.641×10^5 ph/s; and by day 49, the animal developed a tumor of 1-cm diameter with a bioluminescence of 1.94×10^5 ph/s. Animals that were inoculated with 50×10^4 or 500×10^4 cells developed tumors larger than 1-cm diameter before day 49 and were euthanized for histopathological examination.

Histopathological Analysis

Histopathological examination of tumor tissues revealed multiple atypical nuclei and mitotic figures indicative of an aggressive tumor (Fig. 3a). Analyzing signaling modulators in tumor lysates, we detected VEGF expression in J82-Ras-Lux tumor tissues but not in parental cells (Fig. 3b), indicating that VEGF expression, associated with angiogenesis [8], may contribute to tumor development. However, we did not detect any metastatic J82-Ras-Lux tumors by either BLI or histopathological examination.

Discussion

In this communication, we demonstrate that auto-bioluminescent xenograft UBC animal model provided additional benefits of monitoring the entire course of cell inoculation, adaptation, and tumor development to the conventional xenograft animal models of evaluating palpable tumors. Our *in vivo* results indicated a non-linear course of xenograft tumor development; living cells appeared to decline after inoculation, and survived cells regained growth to develop into tumors. Conceivably, an initial adaptation phase was required for inoculated cells to acclimate a new environment, and survived cells continued to develop into tumors [9]. The use of BLI to monitor auto-bioluminescent tumor cells provided an advantage of early detection of xenograft tumor development prior to the presence of palpable tumors in determining xenograft tumor development throughout the course of cell inoculation, adaptation, and tumor growth. In addition, edema and necrotic centers may contribute to the tumor size; thus, measurement of palpable tumors by mechanical calipers may not be reliable until necropsy and histopathological examination are performed for validation.

The sensitivity of bioluminescence detected in cells was reduced *in vivo* than *in vitro*. The sensitivity of BLI may be attenuated by depth of tumor [10, 11] and endogenous chromophores by absorption of bioluminescent signal emitted from cells [12]. Using auto-bioluminescent tumorigenic cells and BLI technique allowed the inoculation of cells, as low as 5×10^4, for studying tumor development and therapeutic intervention. However, our studies revealed variations occurred between individual animals and experiments. For example, in a separate experiment, 3 mice inoculated with 500×10^4 J82-Ras-Lux cells

initially yielded bioluminescence of 6.33×10^5, 5.26×10^5, and 3.28×10^5 ph/s, followed by declined readings of 1.84×10^5, 0, and 0 ph/s around 6 and 8 days; then, animals yielded readings of 1.94×10^5, 0.97×10^5, and 3.19×10^5 ph/s, respectively, by 14 days. Accordingly, this model would be applicable to the advancement of preclinical studies by monitoring auto-bioluminescent tumors prior to a palpable size and performing therapeutic intervention in individuals.

Conclusions

Our research produced, for the first time, a real-time, noninvasive, auto-bioluminescent subcutaneous xenograft UBC animal model for pre-clinical cancer research. Ultimately, the auto-bioluminescent UBC J82-Ras-Lux, J82-Lux, and SW780-Lux cells will be applied to development of orthotopic urinary bladder tumor models by injecting the cells through a catheter into the bladder and using real-time monitoring of tumor development in the bladder, invasion to adjacent tissues, metastasis, regression, and recurrence during the course of therapeutic intervention.

Acknowledgments

References

1. Kim J-B, Urban K, Cochran E, et al. Non-invasive detection of a small number of bioluminescent cancer cells in vivo. PLoS One. 2010; 5:e9364. [PubMed: 20186331]

2. Close DM, Patterson SS, Ripp S, et al. Autonomous bioluminescent expression of the bacterial luciferase Gene cassette (lux) in a mammalian cell line. PLoS One. 2010; 5:e12441. [PubMed: 20805991]

3. Close DM, Xu T, Sayler GS, Ripp S. In vivo bioluminescent imaging (BLI): noninvasive visualization and interrogation of biological processes in living animals. Sensors. 2011; 11:180–206. [PubMed: 22346573]

4. Xu T, Ripp S, Sayler GS, Close DM. Expression of a humanized viral 2 A-mediated lux operon efficiently generates autonomous bioluminescence in human cells. PLoS One. 2014; 9:e96347. [PubMed: 24788811]

5. Buyru N, Tigli H, Ozcan F, Dalay N. Ras oncogene mutations in urine sediments of patients with bladder cancer. J Biochem Mol Biol. 2003; 36:399–402. [PubMed: 12895299]

6. Choudhary S, Wang H-CR. Proapoptotic ability of oncogenic H-Ras to facilitate apoptosis induced by histone deacetylase inhibitors in human cancer cells. Mol Cancer Ther. 2007; 6:1099–1111. [PubMed: 17363503]

7. Choudhary S, Sood S, Donnell RL, Wang H-CR. Intervention of human breast cell carcinogenesis chronically induced by 2-amino-1-methyl-6-phenylimidazo[4,5-b]pyridine. Carcinogenesis. 2012; 33:876–885. [PubMed: 22307971]

8. Goel HL, Mercurio AM. VEGF targets the tumour cell. Nat Rev Cancer. 2013; 13:871–882. [PubMed: 24263190]

9. Maes W, Deroose C, Reumers V, et al. In vivo bioluminescence imaging in an experimental mouse model for dendritic cell based immunotherapy against malignant glioma. J Neuro-Oncol. 2009; 91:127–139.

10. Cui K, Xu X, Zhao H, Wong STC. A quantitative study of factors affecting in vivo bioluminescence imaging. Luminescence. 2008; 23:292–295. [PubMed: 18452141]

11. Zinn KR, Chaudhuri TR, Szafran AA, et al. Noninvasive bioluminescence imaging in small animals. ILAR. 2008; 49:103–115.

12. Vo-Dinh, T. Biomedical photonics handbook. CRC Press; 2003.
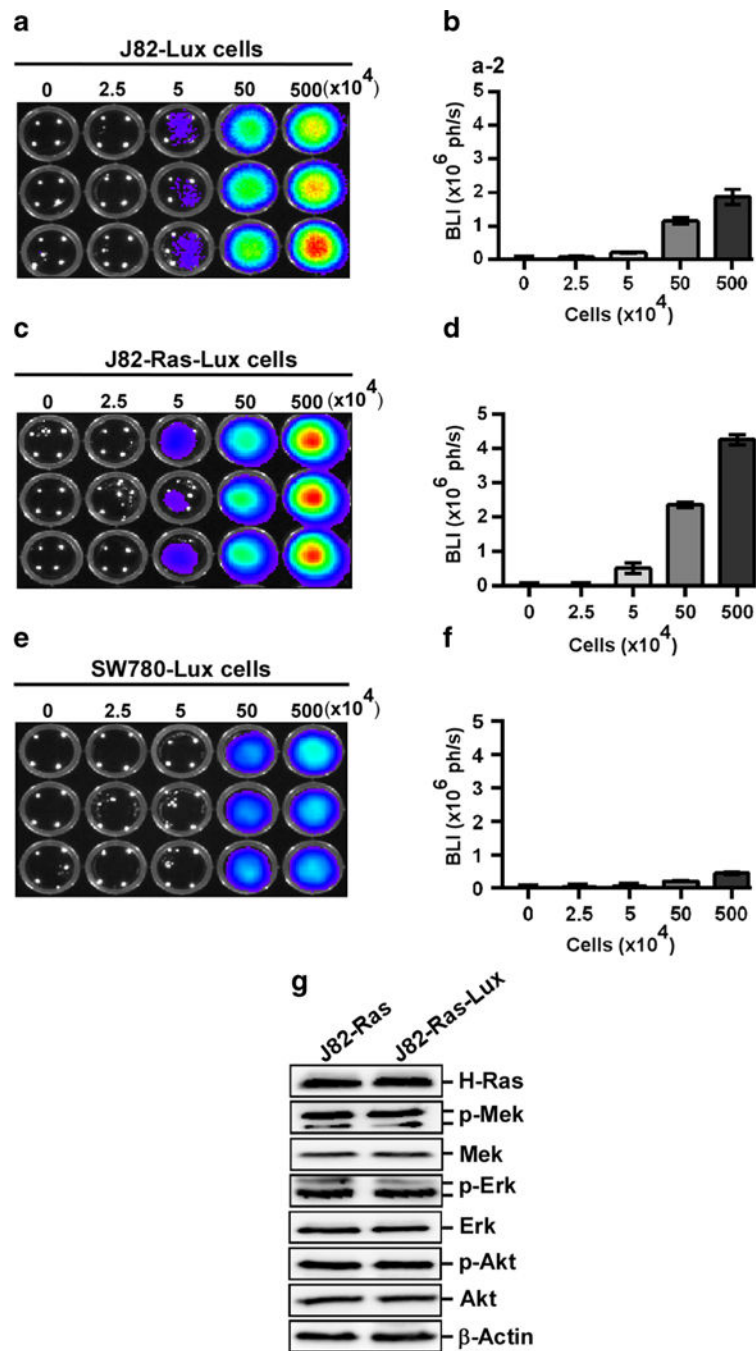
Fig. 1.
Development of auto-bioluminescent cells *in vitro*. **a**, **c**, **e** 0, 2.5, 5, 50, and 500 ($\times 10^4$) J82-Lux, J82-Ras-Lux, and SW780-Lux cells were plated in opaque 96-well plate and imaged with the IVIS Lumina system. **b**, **d**, f BLI (ph/s) signals were quantitated and analyzed. Columns, mean ± SEM of triplicates. **g** Lysates of J82-Ras and J82-Ras-Lux cells were prepared and analyzed by immunoblotting to detect levels of H-Ras, p-Mek, Mek, p-Erk, Erk, p-Akt, and Akt, with β-actin as a control. Data are representative of three independent experiments.
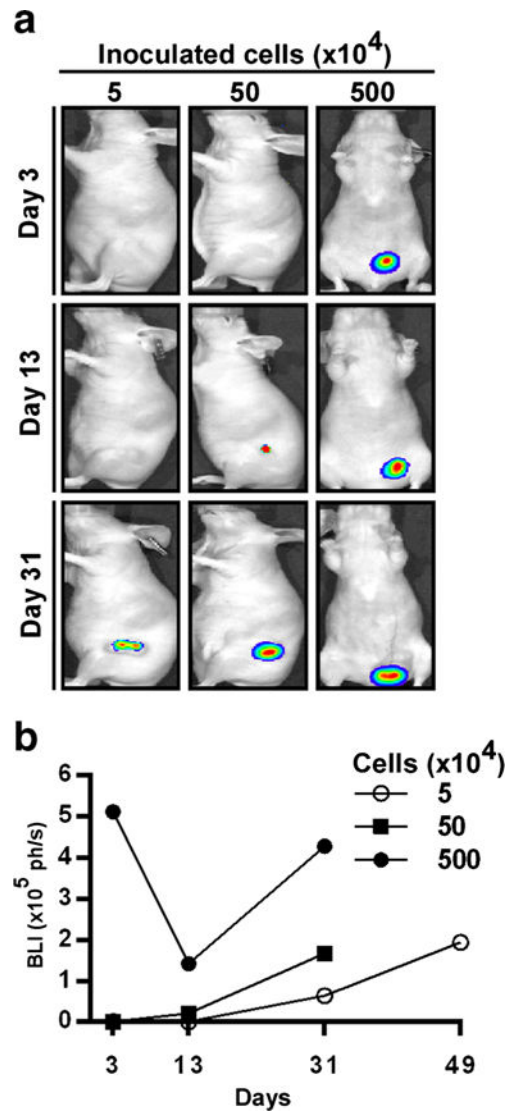
Fig. 2.
Detection of J82-Ras-Lux tumor growth *in vivo*. **a** J82-Ras-Lux cells, at 5, 50, and 500 ($\times 10^4$), were inoculated subcutaneously into nu/nu mice, and BLI was done on days 3, 13, and 31. **b** BLI signals (ph/s) of tumors were quantitated and analyzed to determine tumor development for 49 days.
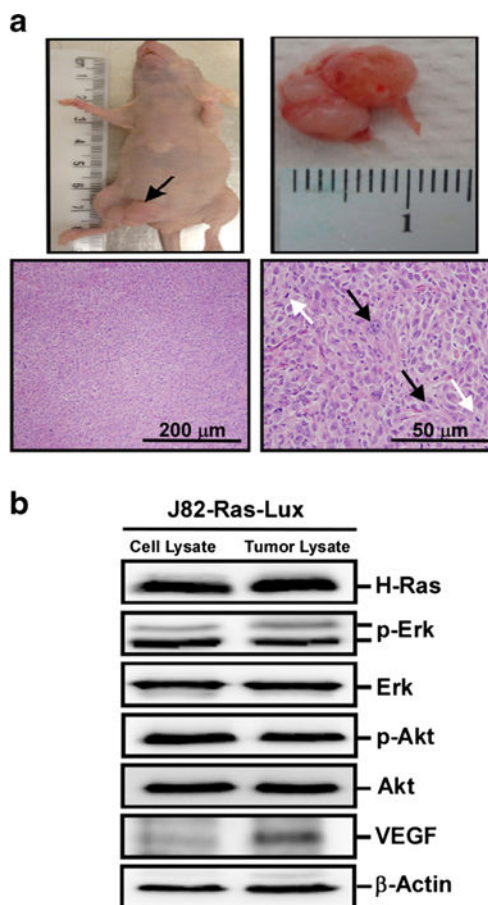
Fig. 3.
Xenograft tumor derived from J82-Ras-Lux cells. The J82-Ras-Lux cells were inoculated subcutaneously into nude mice. **a** *Top left:* xenograft tumors developed in the inoculation site; *top right:* xenograft tumor removed from mouse. *Bottom panels* H&E-stained histological sections revealed neoplastic cells with atypical nuclei (*black arrow*) and mitotic figures (*white arrow*) shown in the right panel. **b** Lysates of J82-Ras-Lux cells and J82-Ras-Lux-derived xenograft tumor tissues were analyzed by immunoblotting using specific antibodies to detect levels of H-Ras, p-Erk, Erk, p-Akt, Akt, and VEGF, with β-actin as a control.